



# Synthesis of a fluorene and quinoxaline-based co-polymer for organic electronics

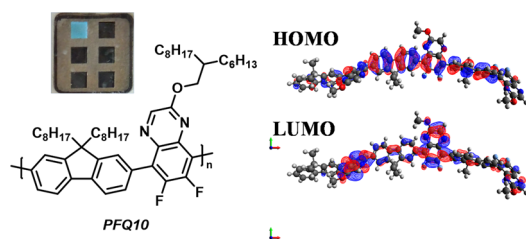
Marco Sigl<sup>1</sup> · Thomas Rath<sup>1</sup> · Bettina Schlemmer<sup>1</sup> · Peter Fürk<sup>1</sup> · Gregor Trimmel<sup>1</sup>

Received: 15 October 2022 / Accepted: 25 December 2022 / Published online: 27 January 2023  
© The Author(s) 2023

## Abstract

Quinoxaline has recently gained interest as monomer in conjugated copolymers because of its easy synthetic accessibility and successful use in highly efficient organic solar cells. In this contribution, we introduce a quinoxaline–fluorene-co-polymer, PFQ10, synthesized by copolymerization of 5,8-dibromo-6,7-difluoro-2-[(2-hexyldecyl)oxy]quinoxaline and 9,9-dioctyl-9H-fluorene-2,7-bis(boronic acid pinacol ester) using the Suzuki–Miyaura reaction. By optimization of the reaction conditions, polymers with molecular weights up to 17.2 kDa and a low dispersity of 1.3 were obtained. PFQ10 showed blue photoluminescence with an emission maximum at 459 nm and a relative fluorescence quantum yield of 0.37. As proof of principle, PFQ10 was employed in organic light-emitting diodes and showed a blue–green electroluminescence.

## Graphical abstract



**Keywords** Polymerizations · Absorption spectra · Density functional theory · Fluorescence · OLED · Polycondensation

## Introduction

Compared to conventional lighting systems, such as incandescent light bulbs, light-emitting diodes (LED) can offer a high performance at lower power consumption [1, 2]. In this regard, organic light-emitting diodes (OLEDs) show a high potential in solid state lighting and flat-panel displays and have come into a considerable research focus since their introduction by Tang et al. in 1987 [3, 4]. Typically, OLEDs consist of a stack of thin films in which the organic light-emitting film is placed between hole and electron injection

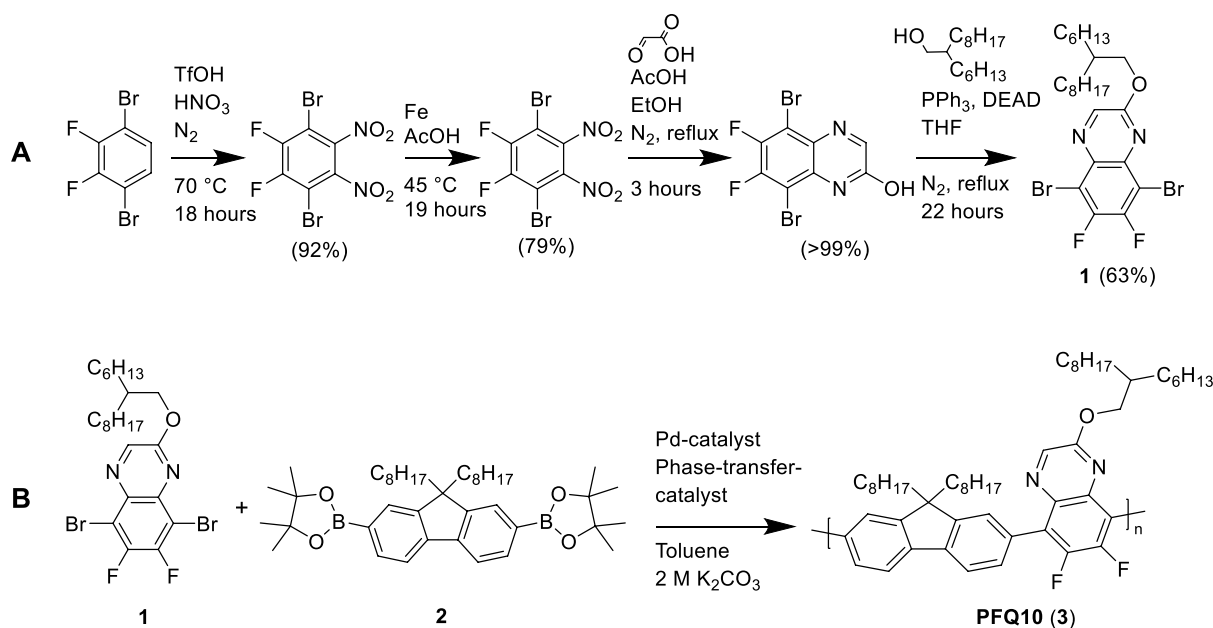
layers and the electrodes. This set-up enables light-weight and flexible devices with low processing costs [5–7].

Small molecules containing quinoxalines have been investigated for the use in OLEDs over the last few years, showing often blue–green luminescence [8–11]. OLEDs with these materials show promise, reaching high photoluminescence quantum yields as well as high external quantum efficiencies [8–16]. Quinoxaline-based materials also show a significant potential as yellow–red thermally activated delayed fluorescence (TADF) or phosphorescent emitters, providing a promising development direction for future research.

Conjugated copolymers are used as organic semiconductors in a variety of applications, such as organic solar cells, organic field effect transistors and OLEDs [3, 5, 17–21]. Moreover, these polymers can be used in photocatalysis and show two-photon absorption, room temperature phosphorescence and TADF [22–24]. The concept of

✉ Gregor Trimmel  
gregor.trimmel@tugraz.at

<sup>1</sup> Institute for Chemistry and Technology of Materials (ICTM), NAWI Graz, Graz University of Technology, Stremayrgasse 9, 8010 Graz, Austria



alternating electron-rich and electron-deficient aromatic building blocks, called (electron-) donor and acceptor units, enables a better intramolecular charge transfer, lowering the respective energy levels and providing a high level of tunability regarding each monomer [21, 25, 26]. Furthermore, polymerization expands the conjugation length, which shifts the highest-occupied molecular orbital (HOMO) and lowest-unoccupied molecular orbital (LUMO) energy levels. This alters the optical properties of the material, like a red-shifted and broadened absorbance as well as improved photosensitization [27–29].

The quinoxaline-based polymer PTQ10, a co-polymer of 6,7-difluoro-2-[(2-hexyldecyl)oxy]quinoxaline and thiophene, is becoming increasingly popular in organic photovoltaics research. Solar cells with PTQ10 as donor reach power conversion efficiencies up to 17% with various non-fullerene acceptors [30, 31]. Additionally, PTQ10 offers a simple preparation, as the quinoxaline monomer can be synthesized in just four straightforward steps from commercially available and cheap starting materials [20, 30].

In this work, the monomeric building block from PTQ10, 5,8-dibromo-6,7-difluoro-2-[(2-hexyldecyl)oxy]quinoxaline (**1**) was combined with 9,9-dioctyl-9H-fluorene-2,7-bis(boronic acid pinacol ester) (**2**), to yield the conjugated co-polymer PFQ10. The products were characterized by NMR, IR, and UV–Vis spectroscopy. The thermal properties were examined via thermogravimetric analysis and differential scanning calorimetry and the frontier molecular orbital energy levels (HOMO, LUMO) were determined by cyclic voltammetry in combination with the

optical bandgap. Finally, the polymer was implemented in OLEDs to evaluate its electroluminescence properties.

## Results and discussion

The synthesis of the quinoxaline monomer (**1**) was performed according to a procedure reported by Rech et al. (Scheme 1), with a similar yield of 45% (<sup>1</sup>H NMR spectrum see Supplementary Information (SI), Fig. S2) [20, 30].

The synthesis of the conjugated co-polymer PFQ10 (poly[(9,9-dioctyl-9H-fluorene-)-alt-(6,7-difluoro-2-(2-hexyl-decyloxy)quinoxaline)], **3**) was performed via Suzuki coupling (Scheme 1B). The fluorene monomer (**2**) was selected as electron-rich aromatic compound because of its donor properties and its facile commercial availability [32]. The Suzuki reaction was optimized regarding the used phase-transfer catalysts, palladium catalysts, and the reaction time. The obtained molecular weights, dispersities, and the reaction yields are summarized in Table 1. The molecular weights were determined from gel permeation chromatography (GPC) with polystyrene as a reference. To obtain a pure product, the crude polymer was precipitated from methanol, followed by subsequent Soxhlet extraction with acetone and CHCl<sub>3</sub>. The CHCl<sub>3</sub> fraction was again precipitated from methanol to obtain the final product.

The highest yields and molecular weights were obtained when using Pd(OAc)<sub>2</sub>/PCy<sub>3</sub> as catalyst and Aliquat 336 as phase-transfer catalyst with a reaction time of 70 h. These conditions were employed with the polymers P–III and P–V

**Table 1** Number-average molecular weights, dispersities, and yields of PFQ10 for different catalysts, phase-transfer catalysts and reaction times

PFQ10 (3)	Catalyst <i>c</i> /mol%	Phase-transfer-catalyst	<i>t</i> /h	$M_n$ /kDa <sup>a</sup>	$\bar{D}$ <sup>a</sup>	Yield/%
P-I	Pd(PPh <sub>3</sub> ) <sub>4</sub> 1.1	Aliquat 336	24	10.7	2.3	27
P-II	Pd(OAc) <sub>2</sub> /PCy <sub>3</sub> 2.0/3.5	TBAF	24	9.07	1.6	23
P-III <sup>b</sup>	Pd(OAc) <sub>2</sub> /PCy <sub>3</sub> 2.2/3.0	Aliquat 336	70	17.2	1.3	32
P-IV	Pd(OAc) <sub>2</sub> /PCy <sub>3</sub> 2.6/3.9	Aliquat 336	24	6.54	1.6	20
P-V	Pd(OAc) <sub>2</sub> /PCy <sub>3</sub> 2.0/3.1	Aliquat 336	70	11.3	1.4	37

<sup>a</sup>Obtained by GPC with polystyrene as reference<sup>b</sup>After 2 h parts of solvent evaporated, which was immediately added again

(see Table 1, entries 3 and 5). The structure was verified with one- and two-dimensional NMR spectroscopy (SI, Figs. S2–S6). The <sup>1</sup>H NMR spectrum showed a characteristic broadening of the peaks compared to those of the monomers.

Employing additional <sup>13</sup>C, COSY, HSQC, and HMBC NMR techniques, all signals except some aliphatic ones of the side chains could be assigned unambiguously. The <sup>1</sup>H NMR spectrum is depicted in Fig. 1 and the <sup>1</sup>H NMR as well as the <sup>13</sup>C NMR shifts are listed in the experimental section. The elemental analysis (C, H, N) agrees very well with the theoretical values with deviations of <0.4% (SI, Table S1).

### Thermal analysis and cyclic voltammetry

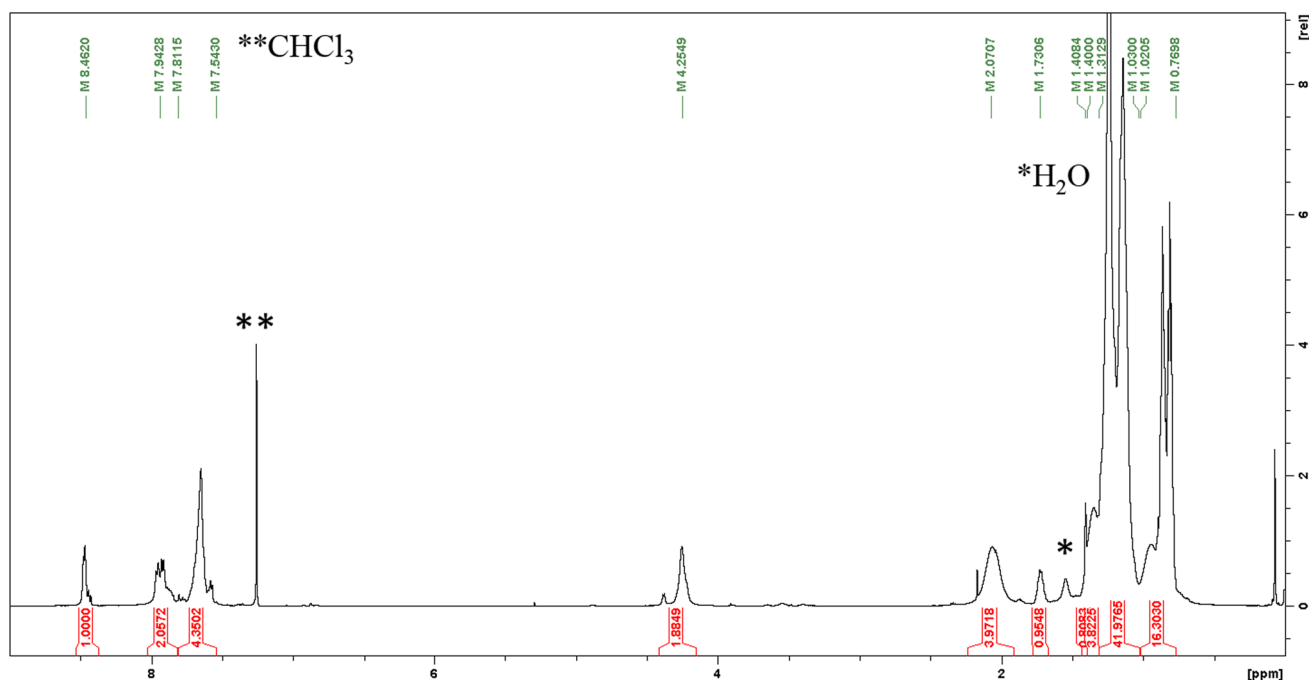
The thermal properties and stability of PFQ10 were analyzed with thermogravimetric analysis (TGA) and differential scanning calorimetry (DSC) at 10 °C min<sup>-1</sup> for both methods. The polymer showed good thermal stability with a

weight loss of 5% at 364 °C. The total weight loss of 55.2% at 525 °C corresponds largely to the thermal decomposition of the side chains of both the fluorene and quinoxaline moieties (Fig. 2a). This agrees well with the theoretical weight loss (56.5%). The DSC analysis showed no discernible transitions in the measured range from 0 to 300 °C (Fig. S9).

For the determination of the HOMO level, cyclic voltammetry (CV) in a 0.1 M (butyl)<sub>4</sub>NPF<sub>6</sub> solution in acetonitrile was performed (Fig. 2b, Table 2). The polymer shows a similarly low HOMO energy of –5.9 eV compared to polymers with similar structures such as polyfluorene (–5.8 eV, [33]), and copolymers of fluorene with unsubstituted quinoxaline (–5.9 eV, [34]), thiophene (–5.7 eV) or dithienyl-benzothiadiazole (–5.6 eV, [35]).

### DFT calculation and orbital simulation

To get insight into the electronic structure of the molecule, density functional theory (DFT) calculations

**Fig. 1** <sup>1</sup>H NMR spectrum and shift assignment to the polymer structure

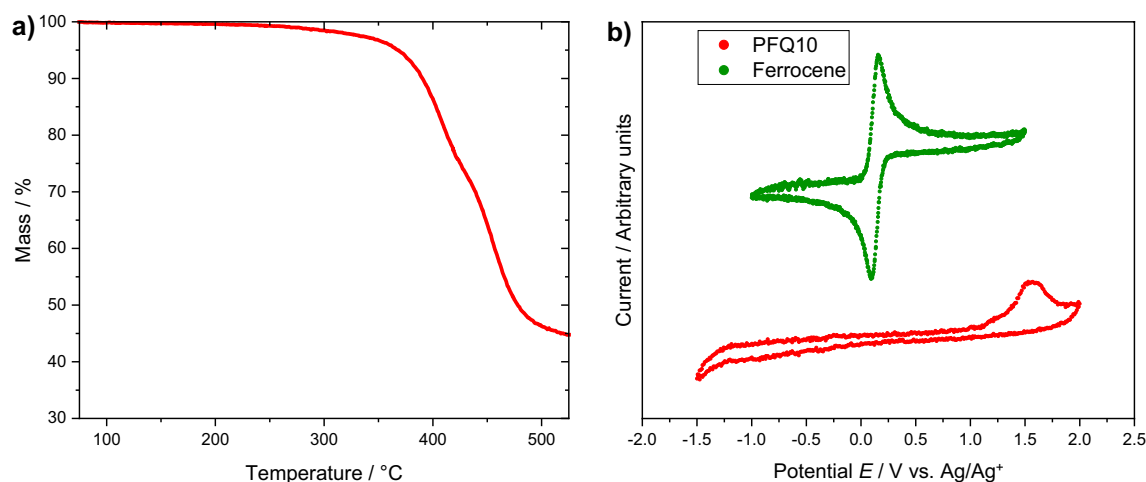


**Fig. 2** a TGA and b CV measurements for HOMO energy ( $-5.9$  eV) determination of PFQ10

**Table 2** Optical and electrical properties of PFQ10 in  $\text{CHCl}_3$

Absorption maximum/nm (absorption coefficient/ $\text{dm}^3$ $\text{mol}^{-1} \text{cm}^{-1}$ )	Emission maximum/nm	Optical bandgap <sup>a</sup> /eV	$E_{el}^{HOMO}$ /eV <sup>b</sup>	$E_{opt}^{LUMO}$ /eV <sup>c</sup>	$\phi_f$ % <sup>d</sup>
337 (17,600)	459	3.0	$-5.9$	$-2.9$	37
370 (18,500)					

<sup>a</sup>The optical bandgap was obtained from the intersection of the absorbance

<sup>b</sup> $E_{el}$  determined via CV measurement

<sup>c</sup> $E_{opt}$  determined with the HOMO energy from the CV and optical bandgap

<sup>d</sup>relative fluorescence quantum yield

were performed on a trimer. To reduce the computing time, the aliphatic side chains were replaced by methyl groups as they do not participate in the conjugated system. The molecule has been geometrically optimized with b3lyp/6-31+G(d,p) (gaussian16) level of theory and the orbital shapes of the HOMO and LUMO were simulated [36]. The computation shows the HOMO to be generally distributed over the whole molecule, while the LUMO is mostly focused on the quinoxaline (acceptor) moieties (Fig. 3). The calculated values in vacuum are with  $-5.4$  and  $-2.0$  eV for the HOMO and LUMO, respectively, significantly higher than those measured ( $-5.9$  and  $-2.9$  eV). On the other hand, the calculations with  $\text{CHCl}_3$  as solvent were significantly better comparable with the measured data, providing values of  $-5.9$  and  $-2.3$  eV for HOMO and LUMO, respectively. The HOMO energy fits very well with the experimental one, but the LUMO energy is still notably higher, which can be explained by the smaller conjugation length as only an oligomer was modeled to reduce the computation time.

## Optical properties

PFQ10 was characterized with UV-Vis absorption and emission spectroscopy (Fig. 4 and Table 2). The polymer absorbs mostly in the upper UV-regime, showing two distinct maxima at 337 ( $\epsilon = 17,600 \text{ mol}^{-1} \text{ dm}^3 \text{ cm}^{-1}$ ) and 370 nm ( $18,500 \text{ mol}^{-1} \text{ dm}^3 \text{ cm}^{-1}$ ).

The polymer solution shows a bright blue fluorescence. The emission showed a maximum at 459 nm, using an excitation wavelength of 370 nm, resulting in a Stokes shift of 89 nm. Using Coumarin-30 as reference [37], the relative quantum yield  $\Phi_f$  of PFQ10 was determined to be 0.37. The absorption of a thin film in the solid state (on a glass substrate) shows a slight red shift (Fig. 4b). Similar to the absorption, the emission showed a notable broadening compared to the solution.

## Organic light-emitting diodes

In a next step, the polymer PFQ10 was incorporated as light-emitting material in OLED devices. For the preparation of the OLEDs, glass/indium tin oxide (ITO) substrates were covered with a thin film of poly(3,4-ethylenedioxythiophene)

**Fig. 3** Chemical structure of the calculated molecule and DFT results of the PFQ10 calculation for the HOMO and LUMO distribution in vacuum. DFT calculation was done with three repeating units at b3lyp/6-31+G(d,p) level of theory. The molecule was calculated both in vacuum and  $\text{CHCl}_3$  environment

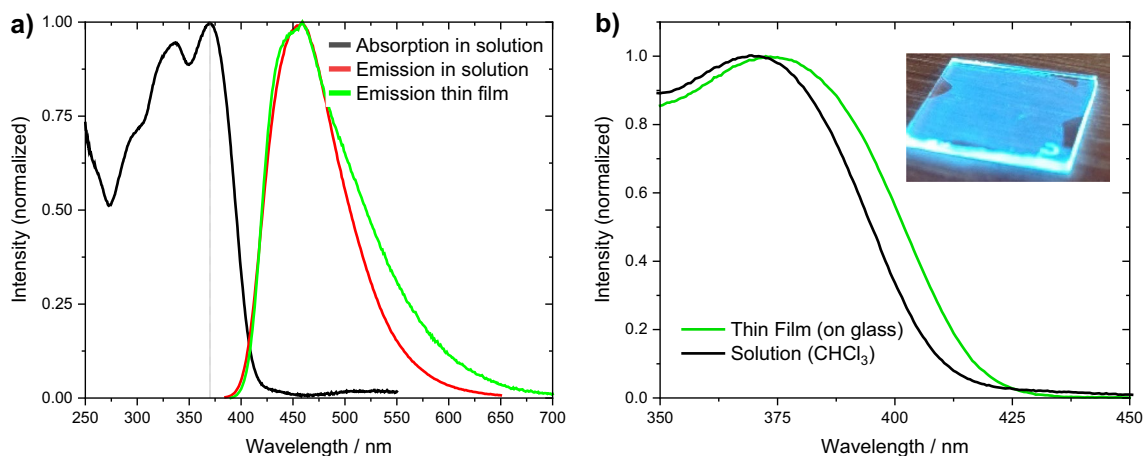
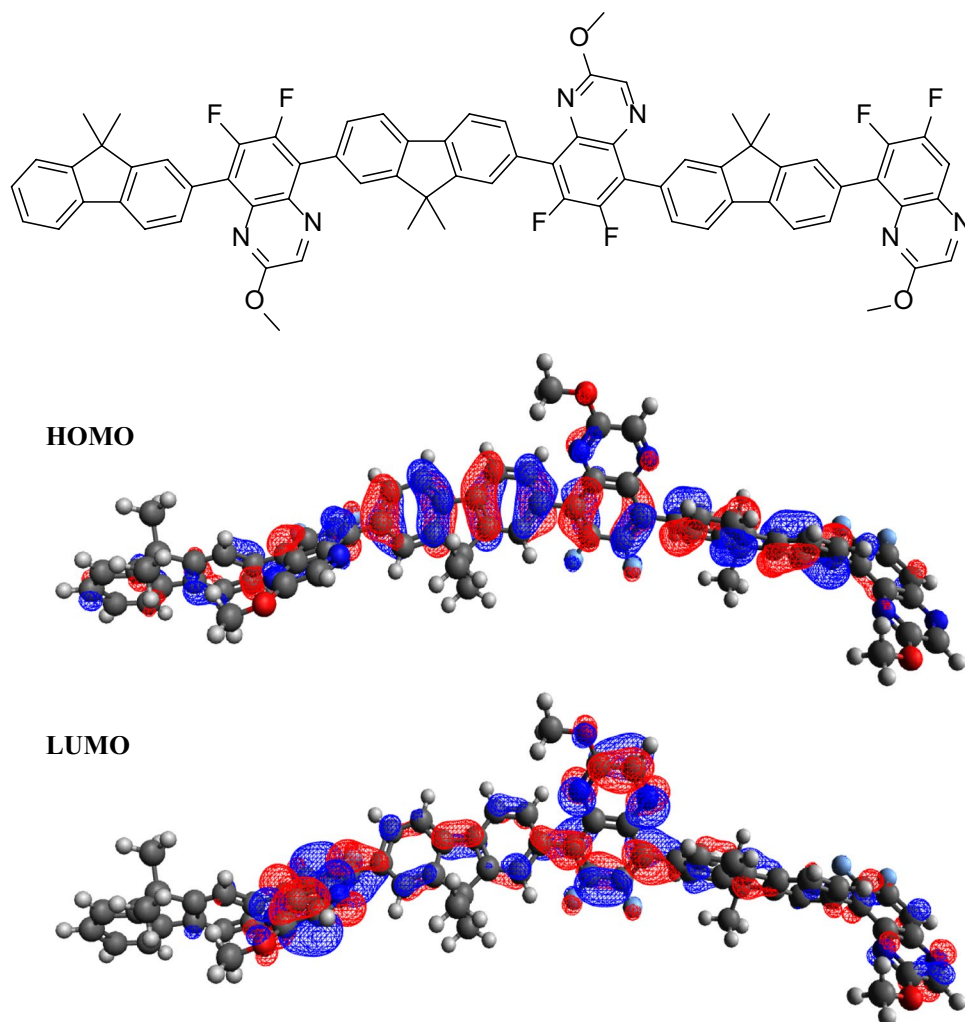
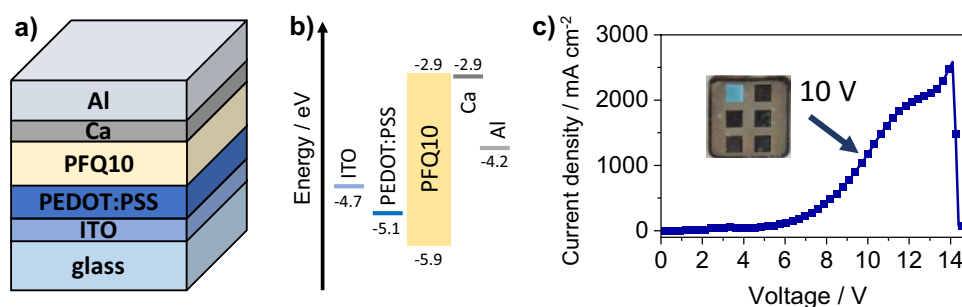


**Fig. 4 a** Normalized absorption and emission spectra (excitation wavelength 370 nm) of PFQ10 in  $\text{CHCl}_3$  solution (red) and thin film (green). **b** Comparison of UV-Vis absorption in solution ( $\text{CHCl}_3$ )

and as thin film on glass. The inset figure shows the photoluminescence of thin-film samples with excitation at 365 nm (color figure online)

**Fig. 5** **a** Device architecture of the OLEDs, **b** schematic energy level diagram of the different OLED layers [21, 38, 39], **c** JV curve of a typical OLED with an area of 0.09 cm<sup>2</sup> (the image shows the electroluminescence at an operating voltage of 10 V)



polystyrene sulfonate (PEDOT:PSS) followed by spin coating of the PFQ10 film (150 nm) from a solution in chlorobenzene.

On top of the active layer, films of calcium and aluminum were deposited as electrodes via thermal evaporation. A scheme of the device architecture and the corresponding energy level diagram are shown in Fig. 5a and b. PEDOT:PSS serves as the hole injection layer [40–42]. The JV characteristic of a typical PFQ10-based OLED is depicted in Fig. 5c. The OLEDs emitted light starting at 9.8 V (visual detection) and the diode is stable up to roughly 11 V before it starts visibly decaying, resulting in an almost complete and irreversible loss of current at around 14 V (Fig. 5c). The inset in Fig. 5c shows an OLED operated at 10 V, which emits blue–green light with CIE<sub>x,y</sub> (Commission Internationale de l’Eclairage) coordinates of  $x=0.26$  and  $y=0.42$ .

## Conclusion

The donor–acceptor type co-polymer PFQ10 was successfully synthesized via Suzuki coupling. The structure was verified with NMR spectroscopy and the material was further characterized regarding its thermal properties, providing a good thermal stability. The polymer shows an absorption maximum at 370 nm and an emission maximum at 459 nm in CHCl<sub>3</sub> with a relative quantum yield of 0.37, with Coumarin-30 as reference. The material was successfully incorporated as light-emitting component in organic light-emitting diodes, yielding blue–green light according to its CIE coordinates with  $x=0.26$  and  $y=0.42$ . This clearly shows that also quinoxaline-based copolymers are promising candidates for luminescent devices.

## Experimental

The chemical reagents and solvents for synthesis and measurements were acquired from commercial sources and used without further purification. For reaction control, TLC plates

with silica gel 60 in aluminum sheets from Merck were used in combination with UV light at 254, 302, and 365 nm. Column chromatography was performed with a Biotage Selekt Flash chromatography system and pre-packed silica gel columns.

<sup>1</sup>H NMR, <sup>13</sup>C NMR, and 2D NMR spectra (COSY, HSQC, HMBC) were recorded using a Bruker Avance 300 MHz and a 500 MHz Inova 500 spectrometer in CDCl<sub>3</sub>. The chemical shifts were referenced to the TMS (0 ppm—<sup>1</sup>H and <sup>13</sup>C NMR) or CHCl<sub>3</sub> (7.26 ppm—<sup>1</sup>H NMR / 77.16 ppm—<sup>13</sup>C NMR) signal.

The UV–Vis absorption spectra were recorded with a Shimadzu UV-1800 spectrometer with an optical quartz glass cuvette and CHCl<sub>3</sub> as solvent. Absorption spectra of thin films were recorded on a CARY 50 UV–Vis spectrometer from Varian and a UV-1800 spectrometer from Shimadzu. Emission spectra were recorded on a Fluorolog-3 luminescence spectrometer equipped with a NIR-sensitive R2658 photomultiplier from Hamamatsu. The FT-IR spectra were recorded with a Bruker ALPHA-p FT-IR spectrometer.

The thermal properties and stabilities were acquired with a STA Jupiter 449C from Netzsch for simultaneous thermal analysis (STA) and a DSC 8500 from Perkin Elmer under N<sub>2</sub> atmosphere for differential scanning calorimetry.

The molecular weights of the polymers were measured with gel permeation chromatography with a modular device from Shimadzu (SPD-20A spectrometer, RID-20A—refractive index detector, CBM-20A—modular system controller, DGU-20A3R-HPLC degassing unit, SIL-20AC autosampler, LC-20AD and a Shimadzu reservoir tray) with polystyrene as standard.

Cyclic voltammetry for the HOMO determination of the polymers was performed with a SP-50 potentiostat from Bio-Logic consisting of a three-electrode set-up. A non-aqueous Ag/AgNO<sub>3</sub> electrode with a 0.1 M AgNO<sub>3</sub> solution in acetonitrile served as reference electrode and a Pt wire as counter electrode. The electrolyte was 0.1 M (butyl)<sub>4</sub>NPF<sub>6</sub> in acetonitrile and the samples were deposited by drop coating from CHCl<sub>3</sub> solutions onto the Pt-disk working electrode. The HOMO was determined with the oxidation onset versus the known Fc/Fc<sup>+</sup> energy level of  $-4.8$  eV below the vacuum level in N<sub>2</sub> atmosphere [43].

Elemental analysis (C, H, N) of the polymers was done with an elemental analyzer vario EI from Elementar Analysensysteme GmbH.

**5,8-Dibromo-6,7-difluoro-2-[(2-hexyldecyl)oxy]quinoxaline (1)** **1** was synthesized according to a procedure reported in literature. 2 cm<sup>3</sup> of fuming nitric acid were added dropwise to 35 cm<sup>3</sup> of triflic acid under N<sub>2</sub> atmosphere and cooled in an ice bath. 4.984 g of 1,4-dibromo-2,3-difluorobenzene (18.3 mmol) was added dropwise. After 2 h the mixture was cooled again and further 4 cm<sup>3</sup> of fuming nitric acid were added. The reaction was heated to 70 °C for 18 h and the yellow precipitate was quenched in stirred pre-cooled (4 °C) water (300 cm<sup>3</sup>) and further stirred for 15 min. The precipitate was filtered with reduced pressure and dried under vacuum (yield: 6.06 g, 92%). 6.06 g of 1,4-dibromo-2,3-difluoro-5,6-dinitrobenzene (16.7 mmol) and 13.06 g of iron powder (234 mmol) were added to a three neck flask under N<sub>2</sub> atmosphere and 175 cm<sup>3</sup> of glacial acetic acid were added. The reaction was heated to 45 °C for 19 h and then cooled to room temperature. A 10 w% NaOH solution was prepared and cooled in an ice bath. The very viscous reaction mixture was poured into the still cooled NaOH solution and the precipitation filtered with a paper filter in a slit sieve plate with slightly reduced pressure via a water jet pump. The yellow-brown precipitate was dissolved in ethyl acetate and washed with saturated NaHCO<sub>3</sub> twice, after which the organic phase was concentrated under reduced pressure. The resulting brown solid was dried overnight under vacuum (yield: 3.93 g, 79%).

1.999 g of 3,6-dibromo-4,5-difluoro-1,2-benzenediamine (6.6 mmol) and 744 mg of glyoxylic acid monohydrate were added to a flask under N<sub>2</sub> atmosphere followed by 10 cm<sup>3</sup> of glacial acetic acid and 10 cm<sup>3</sup> of denatured ethanol (99%). The reaction was heated to reflux for 3 h. The product was extracted with DCM and washed with deion H<sub>2</sub>O. The brown precipitate was filtered from the organic phase which was dried over Na<sub>2</sub>SO<sub>4</sub>. The filtrate was concentrated and recrystallized in ethanol with a few drops of DCM (yield: 2.30 g, > 99%). 2.30 g of 5,8-dibromo-6,7-difluoroquinoxalin-2-ol (6.6 mmol) and 1.990 g of PPh<sub>3</sub> (7.6 mmol) were added to a flask under N<sub>2</sub> atmosphere with 100 cm<sup>3</sup> anhydrous THF. The flask was cooled with an ice bath and 2.02 g of 2-hexyl-1-decanol (7.0 mmol) were added, followed by slow addition of 3.5 cm<sup>3</sup> diethyl azodicarboxylate (8.0 mmol). The reaction was heated to reflux for 22 h, after which the mixture was quenched with deion. H<sub>2</sub>O and extracted with DCM. The organic phase was dried over Na<sub>2</sub>SO<sub>4</sub>, then filtered and the solvents were removed with reduced pressure. The black-brown oil was diluted with very little DCM and OPPh<sub>3</sub> was precipitated by adding about 20 cm<sup>3</sup> of *n*-hexane. The product was purified with column

chromatography (hexane:EA 12:1) and the obtained yellow oil was heated in methanol and frozen at - 18 °C overnight, yielding a white solid (yield: 2.35 g, 63%).

The overall yield of 5,8-dibromo-6,7-difluoro-2-[(2-hexyldecyl)oxy]quinoxaline (**1**) was 45%. [<sup>30</sup>] <sup>1</sup>H NMR (300 MHz, CDCl<sub>3</sub>): δ = 8.51 (s, 1H), 4.49 (d, 2H, *J* = 5.66 Hz), 1.97–1.80 (m, 1H), 1.51–1.14 (m, 24H), 0.95–0.80 (m, 6H) ppm.

**General polymerization procedure of poly[(9,9-dioctyl-9H-9-fluorene)-alt-(6,7-difluoro-2-(2-hexyldecyl)oxy)quinoxaline]** (PFQ10, **3**) The syntheses of the PFQ10 polymers (P-I to P-V) were performed via Suzuki coupling reactions. One equivalent of 5,8-dibromo-6,7-difluoro-2-[(2-hexyldecyl)oxy]quinoxaline (**1**) and 9,9-dioctyl-9H-9-fluorene-2,7-bis(boronic acid pinacol ester) (**2**) were added to a Schlenk flask under N<sub>2</sub> atmosphere. After the respective catalytic system was added (Table 1), deaerated anhydrous toluene was added to reach a monomer concentration of 0.04 mol dm<sup>-3</sup>, followed by 0.7–1.0 cm<sup>3</sup> of deaerated 2 M K<sub>2</sub>CO<sub>3(aq)</sub>. Following the addition of the phase-transfer catalyst, the reaction was heated to reflux for 24–70 h. The reactions were cooled to room temperature after TLC controls (CH/EA 30:1) and taken up in 2–3 cm<sup>3</sup> of CHCl<sub>3</sub> followed by precipitation in 150–200 cm<sup>3</sup> of cold methanol. The voluminous light-yellow precipitate was filtered, washed twice with methanol and further purified with Soxhlet extraction, using acetone and CHCl<sub>3</sub> in succession. The CHCl<sub>3</sub> phase was concentrated under reduced pressure, taken up in 2–3 cm<sup>3</sup> CHCl<sub>3</sub> again and precipitated into 150–200 cm<sup>3</sup> methanol. The collected precipitate was dried in a desiccator over CaCl<sub>2</sub> overnight.

**P-I (3)** The reaction was performed according to the general polymerization procedure. After the addition of 0.15 mmol of each monomer (84.9 mg—**1**, 102.1 mg—**2**), 2.0 mg Pd(PPh<sub>3</sub>)<sub>4</sub> (1.7 μmol, 1.1 mol%) were added as catalyst and one drop of Aliquat 336 was used as phase-transfer catalyst. The reaction was heated for 24 h. With this polymerization, 32 mg (27%) of dried product (**3**) was obtained. *M*<sub>n</sub> = 10.7 kDa, *M*<sub>w</sub> = 24.6 kDa, *M*<sub>w</sub>/*M*<sub>n</sub> = 2.3 (GPC in CHCl<sub>3</sub> vs. PS standard).

**P-II (3)** The reaction was performed according to the general polymerization procedure. After the addition of 0.20 mmol of each monomer (112.9 mg—**1**, 134.3 mg—**2**), 0.93 mg Pd(OAc)<sub>2</sub> (4 μmol, 2 mol%), 1.97 mg PCy<sub>3</sub> (6 μmol, 3.5 mol%) and 0.1 cm<sup>3</sup> of TBAF (1 M in THF) were added. The reaction was heated for 24 h. The dried product (**3**) amounted to 36.1 mg (23%). *M*<sub>n</sub> = 9.07 kDa, *M*<sub>w</sub> = 14.5 kDa, *M*<sub>w</sub>/*M*<sub>n</sub> = 1.6 (GPC in CHCl<sub>3</sub> vs. PS standard).

**P-III (3)** The reaction was performed according to the general polymerization procedure. After the addition of 0.15 mmol of each monomer (84.7 mg—**1**, 101.5 mg—**2**), 0.73 mg Pd(OAc)<sub>2</sub> (3 μmol, 2 mol%) and 1.26 mg PCy<sub>3</sub> (4.5 μmol, 3 mol%) were added as catalyst and one drop of Aliquat 336 was used as phase-transfer catalyst. The reaction was heated for 70 h. The dried product (**3**) amounted to 38.5 mg (32%).  $M_n = 17.2$  kDa,  $M_w = 21.6$  Da,  $M_w/M_n = 1.3$  (GPC in CHCl<sub>3</sub> vs. PS standard).

**P-IV (3)** The reaction was performed according to the general polymerization procedure. After the addition of 0.15 mmol of each monomer (84.7 mg—**1**, 101.4 mg—**2**), 0.88 mg Pd(OAc)<sub>2</sub> (4 μmol, 3 mol%) and 1.63 mg PCy<sub>3</sub> (6 μmol, 4 mol%) were added as catalyst and one drop of Aliquat 336 was used as phase-transfer catalyst. The reaction was heated for 24 h. The dried product (**3**) amounted to 24 mg (20%).  $M_n = 6.5$  kDa,  $M_w = 8.8$  kDa,  $M_w/M_n = 1.4$  (GPC in CHCl<sub>3</sub> vs. PS standard).

**P-V (3)** The reaction was performed according to the general polymerization procedure. After the addition of 0.20 mmol of each monomer (113.1 mg—**1**, 135.8 mg—**2**), 0.92 mg Pd(OAc)<sub>2</sub> (4 μmol, 2 mol%) and 1.75 mg PCy<sub>3</sub> (6 μmol, 3 mol%) were added as catalyst and one drop of Aliquat 336 was used as phase-transfer catalyst. The reaction was heated for 70 h. The dried product (**3**) amounted to 58.5 mg (37%).  $M_n = 11.3$  kDa,  $M_w = 16.1$  kDa,  $M_w/M_n = 1.4$  (GPC in CHCl<sub>3</sub> vs. PS standard).

<sup>1</sup>H NMR (500 MHz, CDCl<sub>3</sub>): δ = 8.46 (s, 1H), 7.94 (m, 2H), 7.54–7.81 (m, 4H), 4.25 (m, 2H), 2.07 (m, 4H), 1.73 (m, 1H), 1.41 (s, < 1 H end group), 1.31–1.40 (m, 4H), 1.03–1.31 (m, 42H), 0.77–1.02 (m, 16H) ppm; <sup>13</sup>C NMR (125 MHz, CDCl<sub>3</sub>): δ = 157.4, 150.9, 140.9, 138.7, 136.5, 134.2, 130.3, 129.9, 125.8, 119.3, 83.6 (only in HMBC), 69.1, 55.3, 40.1, 37.6, 31.9, 31.3, 30.2, 30.1, 29.7, 29.6, 29.4, 29.3, 26.9, 25.0, 24.1, 22.7, 22.6, 14.1 ppm. IR:  $\bar{\nu} = 2952, 2921, 2852, 1599, 1575, 1483, 1459, 1432, 1400, 1375, 1310, 1273, 1208, 1145, 1124, 1100, 1051, 1006, 994, 957$  cm<sup>-1</sup> (SI, Fig. S8). UV–Vis (CHCl<sub>3</sub>,  $c = 4.64 \times 10^{-6}$  mol dm<sup>-3</sup>):  $\lambda_{\max}(\epsilon) = 337.0$  (17,584), 370.5 (18,515) nm (dm<sup>3</sup> mol<sup>-1</sup> cm<sup>-1</sup>).

### OLED fabrication and characterization

Glass/ITO substrates (pre-patterned, Lumtec Luminescence Technology Corp., 15 × 15 mm, 15 Ω/sq) were cleaned by sonication in isopropanol and oxygen plasma treatment (FEMTO, Diener Electronic). Next, a PEDOT:PSS film was applied via spin coating (3500 rpm, 30 s) from a PEDOT:PSS aqueous dispersion (Heraeus Clevious™ P VP AI 4083) filtered through a 0.45 μm polyvinylidene difluoride (PVDF) syringe filter. The films were annealed

under inert conditions (150 °C, 10 min) and layers with a thickness of approx. 30 nm were obtained. PFQ10 was dissolved in chlorobenzene (16 mg cm<sup>-3</sup>) and spin coated onto the PEDOT:PSS film at a spin coating speed of 3000 rpm (150 nm layer thickness), followed by a thermal annealing step at 100 °C for 10 min. A calcium layer (10 nm) and an Al electrode (75 nm) were deposited by subsequent thermal evaporation in high vacuum (ca. 10<sup>-5</sup> mbar) through a shadow mask (3 × 3 mm<sup>2</sup>).

JV characteristics of the OLEDs were recorded in inert nitrogen atmosphere using a Keithley 2400 source meter and a LabView-based software. The color of the OLEDs was analyzed from the digital photographs with the freeware ImageJ to obtain the CIE<sub>x,y</sub> coordinates [44].

**Supplementary Information** The online version contains supplementary material available at <https://doi.org/10.1007/s00706-022-03030-7>.

**Acknowledgements** The authors gratefully acknowledge Ing. Karin Bartl for conducting the STA and GPC measurements and Dipl.-Ing. Reinhold Pommer for conducting the DSC measurement. Furthermore, the authors thank Monika Filzwieser for the elemental analysis, as well as Andreas Russegger MSc for the fluorescence measurement. The authors thank Dr. Petra Kaschnitz for conducting the NMR measurements and greatly supporting their evaluation.

**Funding** Open access funding provided by Graz University of Technology.

**Data availability** Data are available from the corresponding author upon request.

**Open Access** This article is licensed under a Creative Commons Attribution 4.0 International License, which permits use, sharing, adaptation, distribution and reproduction in any medium or format, as long as you give appropriate credit to the original author(s) and the source, provide a link to the Creative Commons licence, and indicate if changes were made. The images or other third party material in this article are included in the article's Creative Commons licence, unless indicated otherwise in a credit line to the material. If material is not included in the article's Creative Commons licence and your intended use is not permitted by statutory regulation or exceeds the permitted use, you will need to obtain permission directly from the copyright holder. To view a copy of this licence, visit <http://creativecommons.org/licenses/by/4.0/>.

### References

1. Humphreys CJ (2011) MRS Bull 33:459
2. Taguchi T (2008) IEEJ Trans 3:21
3. Zhu M, Yang C (2013) Chem Soc Rev 42:4963
4. Tang CW, VanSlyke SA (1987) Appl Phys Lett 51:913
5. Farinola GM, Ragni R (2011) Chem Soc Rev 40:3467
6. D'Andrade BW, Forest SR (2004) Adv Mater 16:1585
7. Misra A, Kumar P, Kamalasanan MN, Chandra S (2006) Semicond Sci Technol 21:R35
8. Wang G, Li J, Li Y, Wang D, Zhang J, Wu Y, Zhen Y, Tang Q, Ma H, Hu W, Wu Z, Jen AKY (2019) J Mater Chem C 7:9690
9. Kim DY, Kang J, Lee SE, Kim YK, Yoon SS (2017) Luminescence 32:1180

10. Joo CW, Huseynova G, Kim JH, Yoo J-M, Kim YH, Cho NS, Lee JH, Kim YH, Lee J (2020) *Thin Solid Films* 695:137753
11. Yin X, Sun H, Zeng W, Xiang Y, Zhou T, Ma D, Yang C (2016) *Org Electron* 37:439
12. Feng Z, Gao Z, Qu W, Yang T, Li J, Wang L (2019) *RSC Adv* 9:10789
13. Wen Z, Yang T, Zhang Di, Wang Z, Dong S, Xu H, Miao Y, Zhao B, Wang H (2022) *J Mater Chem C* 10:3396
14. Gong X, Lu CH, Lee WK, Li P, Huang YH, Chen Z, Zhan L, Wu CC, Gong S, Yang C (2021) *Chem Eng J* 405:126663
15. Xie FM, Zeng XY, Zhou JX, An ZD, Wang W, Li YQ, Zhang XH, Tang JX (2020) *J Mater Chem C* 8:15728
16. Vishwakarma VK, Nagar MR, Lhouvum N, Jou JH, Sudhakar AA (2022) *Adv Optical Mater* 10:2200241
17. Luo D, Jang W, Babu DD, Kim MS, Wang DH, Kyaw AKK (2022) *J Mater Chem A* 10:3255
18. He ZW, Zhang Q, Li CX, Han HT, Lu Y (2022) *Chin J Polym Sci* 40:138
19. Baig N, Shetty S, Al-Mousawi S, Al-Sagheer F, Alameddine B (2018) *Mater Today Chem* 10:213
20. Sun C, Pan F, Bin H, Zhang J, Xue L, Qiu B, Wei Z, Zhang ZG, Li Y (2018) *Nat Commun* 9:743
21. Erlik O, Unlu NA, Hizalan G, Hacioglu SO, Comez S, Yildiz ED, Toppare L, Cirpan A (2015) *J Polym Sci Part A* 53:1541
22. Wu W, Liu B (2022) *Mater Horiz* 9:99
23. Wu W, Feng G, Xu S, Liu B (2016) *Macromolecules* 49:5017
24. Jiang T, Liu Y, Ren Z, Yan S (2020) *Polym Chem* 11:1555
25. Murad AR, Iraqi A, Aziz SB, Abdullah SN, Brza MA (2020) *Polymers (Basel)* 12:2627
26. Yu ZP, Yan K, Ullah W, Chen H, Li CZ (2021) *ACS Appl Polym Mater* 3:60
27. Tsuda A, Osuka A (2001) *Science* 293:79
28. Wu W, Mao D, Xu S, Kenry HF, Li X, Kong D, Liu B (2018) *Chemistry* 4:1937
29. Liu B, Zhang H, Liu S, Sun J, Zhang X, Tang BZ (2020) *Mater Horiz* 7:987
30. Rech JJ, Neu J, Qin Y, Samson S, Shanahan J, Josey RF, Ade H, You W (2021) *Chemsuschem* 14:3561
31. Chang Y, Zhang J, Chen Y, Chai G, Xu X, Yu L, Ma R, Yu H, Liu T, Liu P, Peng Q, Yan H (2021) *Adv Energy Mater* 11:2100079
32. Liu Z, Zhang L, Gao X, Zhang L, Zhang Q, Chen J (2016) *Dyes Pigm* 127:155
33. Neher D (2001) *Macromol Rapid Commun* 22:1365
34. Wen D, Fu YY, Shi LQ, He C, Dong L, Zhu DF, He QG, Cao HM, Cheng JG (2012) *Sens Actuators B Chem* 168:283
35. Jin JK, Choi JK, Kim BJ, Kang HB, Yoon SC, You H, Jung HT (2011) *Macromolecules* 44:502
36. Frisch MJ, Trucks GW, Schlegel HB, Scuseria GE, Robb MA, Cheeseman JR, Scalmani G, Barone V, Petersson GA, Nakatsuji H, Li X, Caricato M, Marenich AV, Bloino J, Janesko BG, Gomperts R, Mennucci B, Hratchian HP, Ortiz JV, Izmaylov AF, Sonnenberg JL, Williams-Young D, Ding F, Lipparini F, Egidi F, Goings J, Peng B, Petrone A, Henderson T, Ranasinghe D, Zakrzewski VG, Gao J, Rega N, Zheng G, Liang W, Hada M, Ehara M, Toyota K, Fukuda R, Hasegawa J, Ishida M, Nakajima T, Honda Y, Kitao O, Nakai H, Vreven T, Throssell K, Montgomery JA, Jr, Peralta JE, Ogliaro F, Bearpark MJ, Heyd JJ, Brothers EN, Kudin KN, Staroverov VN, Keith TA, Kobayashi R, Normand J, Raghavachari K, Rendell AP, Burant JC, Iyengar SS, Tomasi J, Cossi M, Millam JM, Klene M, Adamo C, Cammi R, Ochterski JW, Martin RL, Morokuma K, Farkas O, Foresman JB, Fox DJ (2019) *Gaussian 16, Revision C. 01*. Gaussian, Inc, Wallingford CT
37. Senthilkumar S, Nath S, Pal H (2004) *Photochem Photobiol* 80:104
38. Liu G, Liu Z, Wang L, Xu C, Wu S, Xie X (2022) *Org Electron* 107:106565
39. Li R, Liu G, Xiao M, Yang X, Liu X, Wang Z, Ying L, Huang F, Cao Y (2017) *J Mater Chem A* 5:23926
40. Griesser T, Rath T, Stecher H, Saf R, Kern W, Trimmel G (2007) *Monatsh Chem* 138:269
41. Kim M, Kwon BH, Joo CW, Cho MS, Jang H, Kim YJ, Cho H, Jeon DY, Cho EN, Jung YS (2022) *Nat Commun* 13:75
42. Kamtekar KT, Monkman AP, Bryce MR (2010) *Adv Mater* 22:572
43. Murugesan V, de Bettignies R, Mercier R, Guillerez S, Perrin L (2012) *Synth Met* 162:1037
44. Abramoff MD, Magalhaes PJ, Ram SJ (2004) *Biophotonics Int* 11:36

**Publisher's Note** Springer Nature remains neutral with regard to jurisdictional claims in published maps and institutional affiliations.